

# Mechanical and Fracture Behavior of an Artificially Ultraviolet-Irradiated Poly(ethylene-carbon monoxide) Copolymer

J. Abanto-Bueno, J. Lambros

*Aerospace Engineering Department, University of Illinois at Urbana-Champaign, Urbana, Illinois 61801*

Received 12 March 2003; accepted 3 October 2003

**ABSTRACT:** In this work, 1 wt % carbon monoxide (CO) poly(ethylene-carbon monoxide) (ECO) copolymer sheets were artificially exposed to ultraviolet (UV) light with a power density of 3 mW/cm<sup>2</sup> for up to 130 h. A thorough mechanical characterization of the irradiated material was conducted, in which both the stress-strain data and the values of the quasistatic crack initiation and growth toughness were measured and correlated with companion uniaxial tensile tests and single-edge-notched fracture tests. Average values of the elastic modulus, failure strain, and failure stress were determined from the tensile tests. The full-field optical technique of digital image correlation was used to quantify in-plane deformation (displacements and displacement gradients) during the fracture experiments and to extract values of the crack initiation and growth fracture toughness. The elastic modulus increased monotonically

with UV irradiation for the exposure times used in this investigation. In addition, for low irradiation times of less than 5 h, both the failure strain and failure stress of ECO decreased, and this caused a corresponding decrease in the crack initiation and growth toughness. However, for longer irradiation times, the failure strain remained almost invariable, whereas the failure stress increased by about 25% over that of unirradiated ECO. As a result, for longer irradiation times (>5 h), 1 wt % CO ECO became not only stiffer but also stronger and tougher, as quantified by companion fracture experiments. © 2004 Wiley Periodicals, Inc. *J Appl Polym Sci* 92: 139–148, 2004

**Key words:** ECO; photodegradation; mechanical properties; fracture; toughness

## INTRODUCTION

Poly(ethylene-carbon monoxide) (ECO) is a semicrystalline copolymer that forms part of the special class of enhanced degradable polymers,<sup>1</sup> which are designed specifically to exhibit accelerated mechanical degradation when exposed to ultraviolet (UV) light. Such mechanical degradation makes these polymers environmentally friendly materials because they are expected to break down into smaller nontoxic parts under the effects of environmental forces such as wind, rain, and light. ECO is engineered by the random addition of small and known amounts of photosensitive carbonyl groups [carbon monoxide (CO) ketones] to the backbone chain of low-density polyethylene and thus shows a polyketonic structure  $[-(\text{CH}_2\text{CH}_2)_n-(\text{CO})-]$ . It is mostly used as disposable packing, such as six-pack ring carriers.

The complex process of photolysis of ECO has been studied extensively and is chemically and physically

understood.<sup>2–6</sup> The carbonyl groups absorb UV light, and this causes Norris type I and type II chemical reactions (typical of ketones), which result in a reduction of the copolymer molecular weight, competition between the processes of main-chain scission and crosslinking, the evolution of CO and vinyl groups, and an increase in the crystalline region. The carbonyl concentration of thick sheets of LPDE under natural and artificial UV irradiation was studied by Furneaux et al.<sup>7</sup> The carbonyl concentration increased with the UV-irradiation time but remained relatively constant for every UV-irradiation period, up to a depth of 0.8 mm, decreasing rapidly with increasing depth. Therefore, LPDE sheets 0.8 mm thick or thinner would undergo uniform photooxidation through their thickness.

Several studies have also been conducted to determine the effect of UV light on the macroscopic mechanical properties of ECO. These, however, have centered on evaluating the uniaxial failure strain and elastic modulus, both of which have been observed to depend on UV-light exposure. The initially very ductile ECO becomes increasingly more brittle with the UV-irradiation time: the failure strain decreases, mostly during early irradiation times,<sup>1,8</sup> and the elastic modulus increases, with shorter wavelengths (<328

Correspondence to: J. Lambros (lambros@uiuc.edu).

Contract grant sponsor: National Science Foundation; contract grant number: CMS 01-15954.

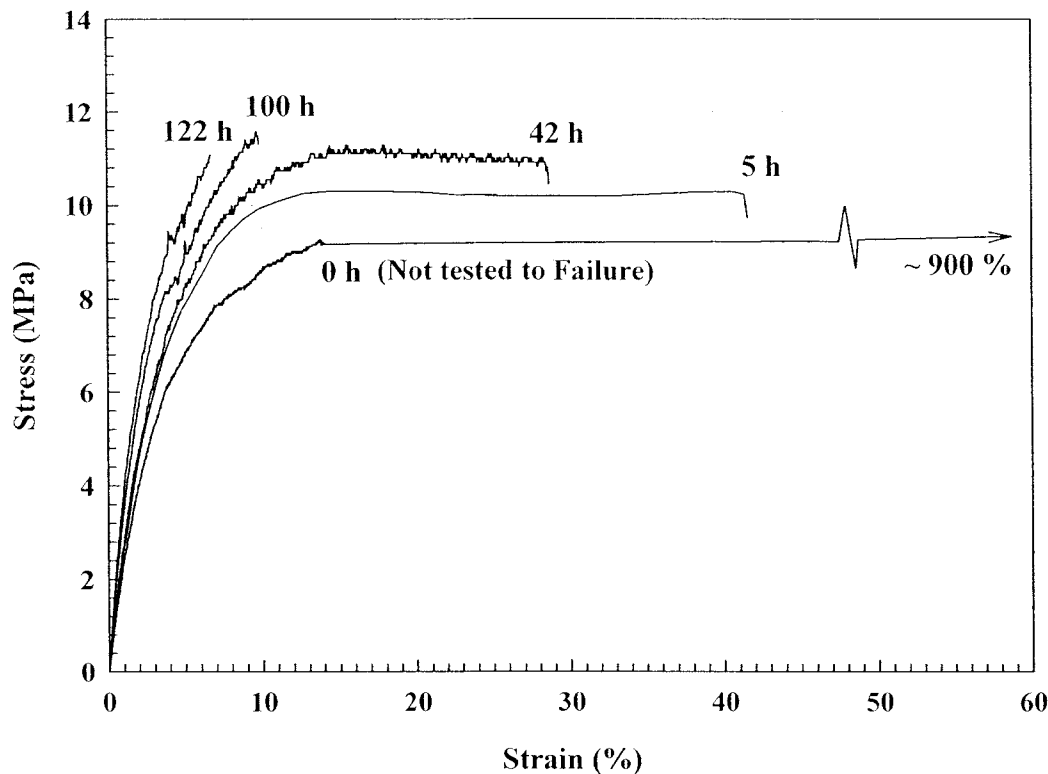


**Figure 1** Effect of the UV-irradiation time on the stress-strain behavior of ECO reported by Lambros et al.<sup>11</sup> The value of the failure strain for unirradiated ECO (900%) was taken from the literature.<sup>9</sup>

nm) being primarily responsible for this photodegradation.<sup>9</sup> Exploiting this behavior, and motivated by the work of Li et al.,<sup>10</sup> Lambros et al.<sup>11</sup> developed a simple and inexpensive technique for the fabrication of laboratory-scale graded materials by gradually altering the mechanical properties of ECO through selective UV irradiation. Figure 1 shows uniaxial stress-strain curves obtained by Lambros et al.<sup>11</sup> for ECO irradiated at different times. The continuous increase in the stiffness and decrease in the failure strain are evident; the failure stress, however, is approximately constant after a brief increase at very short irradiation times.

By the extension of these results, the fracture toughness of ECO is expected to degrade with increasing irradiation time, and this adds to its environmentally friendly behavior. However, only very limited fracture toughness data on ECO are available in the literature. Ivanova et al.<sup>12</sup> presented fracture work measurements for ECO irradiated at three times (24, 48, and 96 h); however, no crack propagation data were given. More recently, in the work of Li et al.,<sup>13</sup> limited information on crack growth resistance curves in irradiated ECO was provided: a hybrid experimental/numerical method, in which boundary load measurements in conjunction with a finite element analysis were used, provided crack growth resistance curves

for ECO at three different irradiation times. Figure 2 shows these crack growth resistance curves, that is, the stress intensity factor ( $K_I$ ) versus the crack extension ( $\Delta a$ ), for irradiation times of 5, 60, and 106 h, and a monotonic decrease in toughness can be seen.

From the aforementioned studies, it can be seen that ECO has applications both as a commercial environmentally friendly disposable packing product and as a model material for studying the mechanical behavior of complex heterogeneous systems. However, in both areas, a more detailed understanding of the mechanical property changes in this material when exposed to UV light is needed. For instance, in the case of a disposable packing product, it is expected that, after its short use, the material will break down into smaller pieces because of environmental forces, principally UV light. This depends not only on the material stiffness and failure strain degradation but also on the evolution of crack initiation and growth fracture toughness. Therefore, the principal objective of this work is to study in detail the mechanical degradation of ECO under the effect of UV irradiation with special emphasis placed on (1) the accurate determination of crack initiation and growth fracture toughness (i.e., the resistance curve) with state-of-the-art measurements techniques and (2) the direct linking of the fracture response to detailed measurements of the

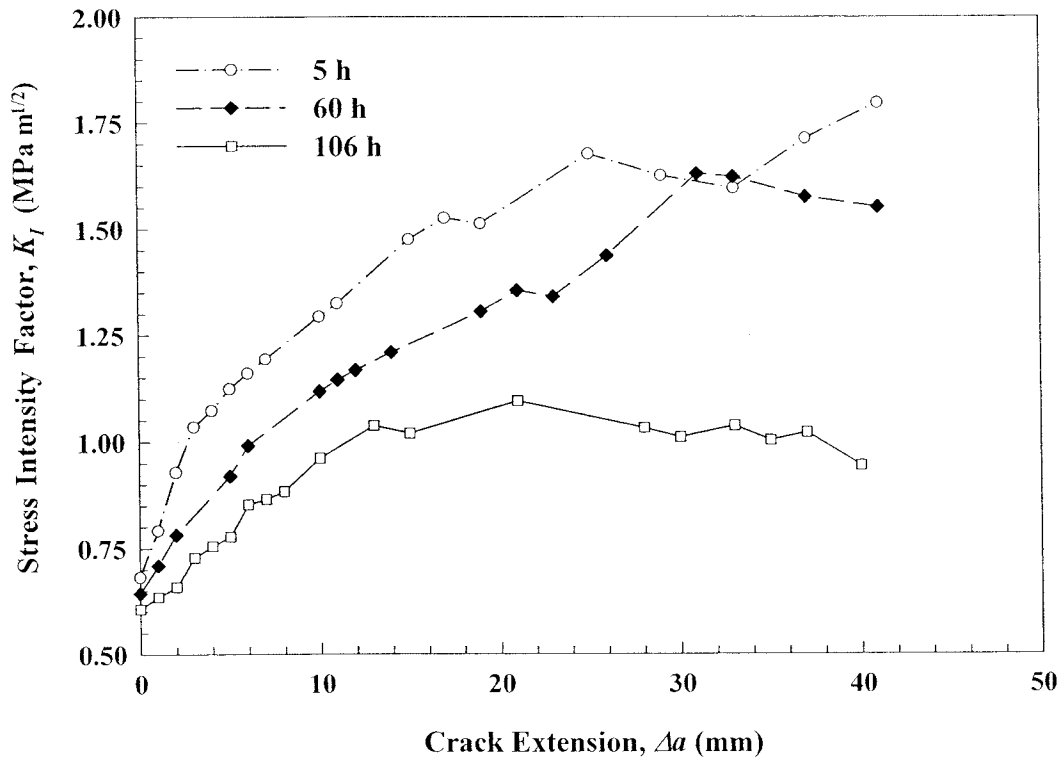


Figure 2 Effect of the UV-irradiation time on the fracture behavior of ECO reported by Li et al.<sup>13</sup>

stiffness, failure strain, and failure stress for the material.

### EXPERIMENTAL

The material used in this investigation was in the form of thin sheets (nominal thickness = 406  $\mu\text{m}$ ) of ECO containing 1 wt % CO. The material was provided by the Hi-Cone Division of Illinois Tools Works, Inc. (Chicago, IL), which also provided the material for the study of Lambros et al.<sup>11</sup> and Li et al.,<sup>13</sup> although the material in this study was acquired 3 years later. The first step of this study was to measure the fundamental mechanical and physical properties of the as-received (unirradiated) ECO sheets. The measured material properties are presented in Table I. The elastic modulus, failure strain, and failure stress were determined from uniaxial tensile tests. The dynamic Poisson's ratio ( $\nu_d$ ) was determined from ultrasonic measurements of both the elastic dilatational ( $c_d$ ) and shear ( $c_s$ ) wave speeds with the following relation:

$$\nu_d = \frac{1 - 2\left(\frac{c_s}{c_d}\right)^2}{2 - 2\left(\frac{c_s}{c_d}\right)^2} \quad (1)$$

For comparison, the static value of the static Poisson's ratio of ECO has been reported in the literature to be

0.45.<sup>14</sup> The density of unirradiated ECO was determined from the average ratio of the mass and volume of 10 samples with different dimensions. Finally, the melting temperature and glass-transition temperature were determined with differential scanning calorimetry (DSC; DSC821<sup>e</sup> measuring module, Mettler-Toledo, Inc., Columbus, OH) at a 10°C/min heating rate.

The UV irradiation of ECO was performed artificially with a dual UV fluorescent table (Cole-Parmer Instrument Co., Vernon Hills, IL) as a light source. This table used six fluorescent tubes that, in combination with a filter (400 mm  $\times$  200 mm), emitted, almost uniformly, UV light at a wavelength of 254 nm, which was within the range needed to achieve considerable mechanical degradation of ECO.<sup>9</sup> The uniformity of the resulting irradiation was verified with a short-

TABLE I  
Measured Mechanical and Physical Properties of Unirradiated ECO

Material property	Average value
Elastic modulus (MPa)	178
Failure strain (%)	>360
Failure stress (MPa)	9.25
$\nu_d$	0.426
Density (kg/m <sup>3</sup> )	960
Melting temperature (°C)	115
Glass-transition temperature (°C)	41

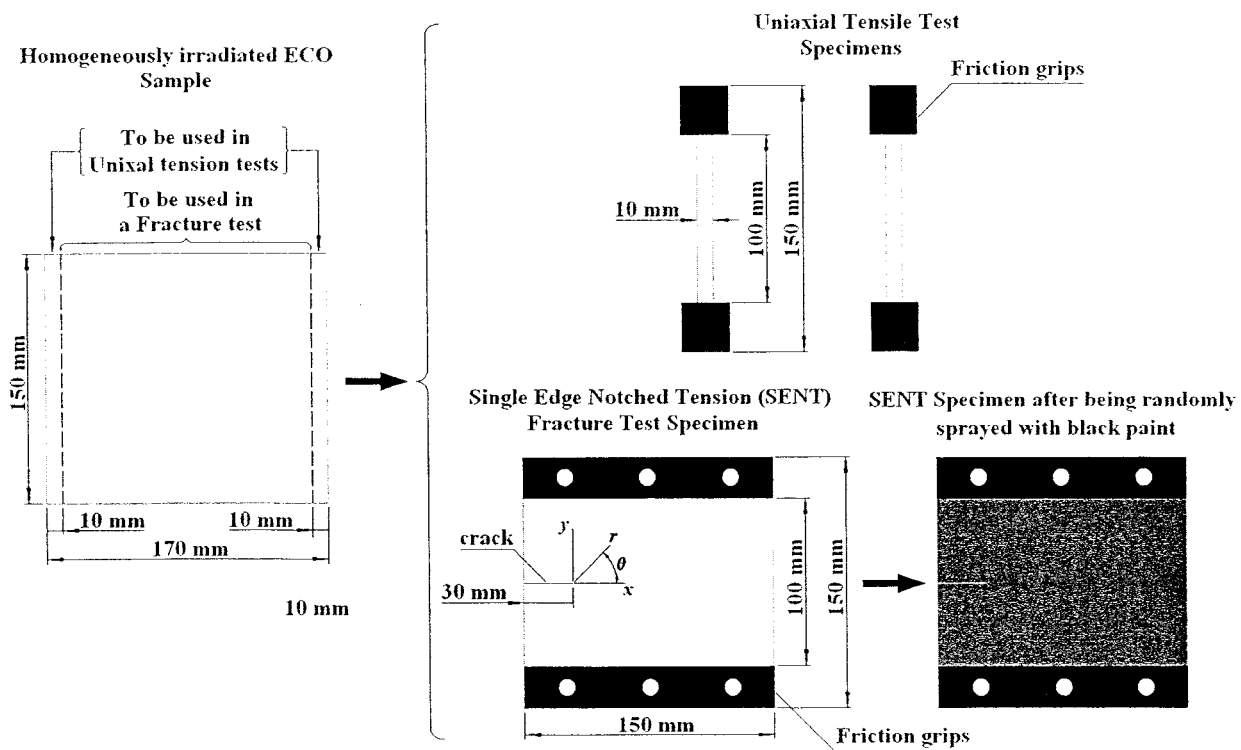


**Figure 3** Initial dimensions of the irradiated ECO sheet and the final dimensions and geometry of the tensile and fracture specimens obtained from it. The coordinate system (centered at the crack tip) used in the analysis of the post-fracture experiments is also shown.

wave UV intensity meter (Cole-Parmer Instrument). The power density was found to be  $3 \pm 0.2 \text{ mW/cm}^2$  over the entire  $400 \text{ mm} \times 200 \text{ mm}$  irradiation area. This measurement was repeated before the irradiation of each specimen to ensure the consistent intensity of the irradiation for all the samples. If the power density fell below a value of  $2.8 \text{ mW/cm}^2$ , the lamps in the UV table were replaced. This usually took place after 800 h of irradiation. Samples of initially unirradiated ECO sheets with dimensions of  $300 \text{ mm} \times 170 \text{ mm}$  were placed on an aluminum plate at a distance of 35 mm directly below the UV source and were homogeneously irradiated for different periods of time: 0.25, 0.5, 1, 1.5, 2, 3, 5, 42, 100, and 130 h. The thickness of the sample ( $406 \mu\text{m}$ ) was small enough to ensure uniform irradiation through the thickness.<sup>7</sup> The irradiated sheets were then cut in half to obtain two identical samples ( $170 \text{ mm} \times 150 \text{ mm}$ ) for every irradiation period. For control over any thermal or moisture effects, all irradiated samples were immediately placed in a refrigerator, the temperature and relative humidity of which were kept at  $50 \pm 2 \text{ }^\circ\text{F}$  and  $50 \pm 2\%$ , respectively. Particles of drierite (anhydrous calcium sulfate) were also used to maintain a dry atmosphere inside the refrigerator. The irradiated samples were left inside the refrigerator for approximately 3 days before being tested.

The irradiated ECO samples ( $170 \text{ mm} \times 150 \text{ mm}$ ) were used to perform two sets of companion experiments: uniaxial tensile tests and fracture tests. The final geometry of every irradiated ECO sample allowed us to obtain three specimens: two strip specimens for use in uniaxial tensile tests and a sheet for use in a fracture experiment. Figure 3 shows the initial dimensions of the irradiated ECO sample and the final dimensions and geometry of the three specimens obtained from it. Using tensile and fracture specimens from the same sheet of material allows for a direct comparison between the constitutive and fracture results and also provides a method for reducing the effects of material variability, which is significant in ECO.<sup>1,9,11,12</sup>

Specimens used in the uniaxial tensile tests (see Fig. 3) were cut from the irradiated ECO sample with a sharp blade. The tensile tests were carried out in a universal testing machine (RT/30, MTS System Corp., Eden Prairie, MN) under displacement control conditions (constant machine crosshead speed =  $0.5 \text{ mm/min}$ ). A 100-lb load cell (Transducer Techniques, Inc., Temecula, CA) was used to measure the applied load. Friction grips made of 3M aluminum abrasive paper (grade 150) were placed between the specimen and the machine grips to prevent specimen sliding in the grips. The universal testing software package

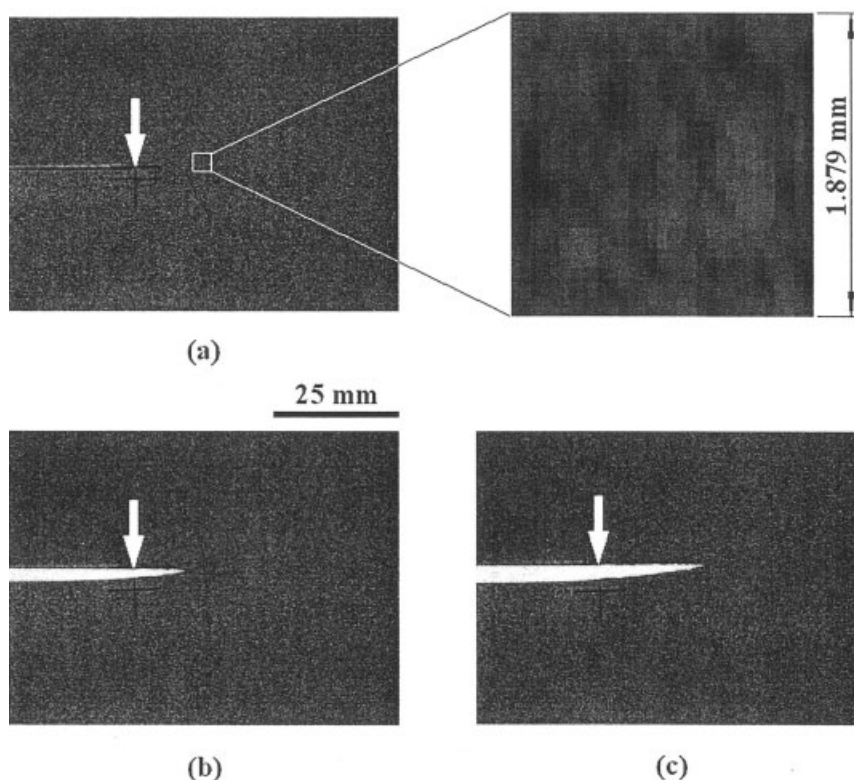


**Figure 4** Selected sequence of digital images taken from the fracture experiment of an ECO specimen irradiated for 42 h. A white arrow indicates the original crack-tip position. The time ( $t$ ), crack length ( $a$ ), and applied displacement ( $V_0$ ) were as follows: (a)  $t = 0$  s,  $a = 30$  mm, and  $V_0 = 0$  mm (undeformed configuration); (b)  $t = 330$  s,  $a = 39.64$  mm, and  $V_0 = 2.75$  mm; and (c)  $t = 394$  s,  $a = 50.06$  mm, and  $V_0 = 3.28$  mm.  $a$  was measured directly from the images. The blowup in Figure 4(a) shows a speckle pattern detail over a 31 pixel  $\times$  31 pixel subset.

TestWorks 4 (MTS System) was used to control the testing machine, acquire the machine crosshead displacement and resulting applied load signals, and perform post-test analysis. Because the compliance of the testing machine frame (5.7 nm/N) could be neglected in comparison with that of unirradiated and irradiated ECO for the maximum applied load (<50 N), the strain was determined from the machine crosshead displacement directly. The elastic modulus was determined with straight-line least-square fitting of the raw data of the elastic region.

Single-edge-notched tension specimens with an initial crack length of 30 mm (cut with a sharp blade) were used in the fracture tests, which were also conducted under displacement control conditions and mode I (symmetric) loading. Before the fracture experiment, one surface of the specimen was sprayed with black paint with an airbrush to create a random speckle pattern (see Fig. 3). Such a pattern was needed to measure the in-plane deformation of the specimen during the fracture tests with the full-field digital image correlation (DIC) technique. The DIC technique is a versatile and accurate method of measuring full-field in-plane displacements and displacement gradients through the comparison of a pair of digital im-

ages of the speckled surface of the specimen before and after deformation. This technique is easy to implement because it only requires a digital charge-coupled device (CCD) camera and a computer to record the entire fracture test. Detailed information on this technique is available in the literature<sup>15-18</sup> and is not given here for the sake of brevity.

The same loading rate used in the uniaxial tension tests was used so that any rate-dependence effects would be minimized (Lambros et al.<sup>11</sup>) and a direct comparison between the tensile and fracture responses could be made. A uniform displacement along the upper grip was applied in the positive  $y$  direction (see Fig. 3), whereas the lower grip was held fixed. The applied displacement and resulting applied load signals were recorded. During the fracture tests, a Sony IEEE 1394 digital CCD with 1280 pixel  $\times$  960 pixel resolution (model XCD-SX900, Unibrain, Inc., San Ramon, CA) was used to take pictures every 2 s of the region surrounding the growing crack. The data were directly stored in a 120-GB, 7200-rpm external hard drive allowing for continuous recording of up to 12.4 h, if needed. Figure 4 shows a selected sequence of such digital pictures corresponding to the fracture test of a 42-h-irradiated ECO specimen. The blowup of

Figure 4(a) shows the speckle pattern detail over a 31 pixel  $\times$  31 pixel subset used in the DIC technique.

## RESULTS AND DISCUSSION

### Tensile tests

A set of uniaxial stress–strain curves obtained from the tensile tests is shown in Figure 5(a). For a better assessment of the mechanical changes during larger irradiation periods, the region corresponding to lower strain levels (<20%) has been enlarged and is also shown. Curves corresponding to irradiation times of 0.25, 1.5, 2, and 3 h are not shown to avoid gross overlapping, but they also follow the trends shown. At least three specimens were tested for every irradiation time. From these tests, average values of the elastic modulus, failure strain, and failure stress were extracted, and they are presented as a function of the UV-irradiation time in Figure 5(b). The error bars plotted in Figure 5(b) represent scatter from nominally identical experiments. For points that do not possess error bars, the scatter was smaller than the symbols used in the plot (<2%). The biggest scatter bands are on the failure strain for lower irradiation times because this is the time of greatest sensitivity to UV irradiation. From Figure 5(a,b), it is clear that overall UV-light exposure drastically affects the mechanical response of ECO, as reported in previous investigations.<sup>1,8,9–13</sup> The elastic modulus increases with the irradiation time and after 130 h of irradiation attains a value about 2.15 times larger than that of the unirradiated one. The failure strain decreases sharply during early irradiation times (<5 h), after which time it remains approximately constant (ca. 10%) for the periods of UV irradiation used here. However, comparing these results with previous studies (e.g., see Fig. 1 from Lambros et al.<sup>11</sup>), we can see one important difference: the failure stress increases for longer irradiation times, attaining a value approximately 25% (130 h) greater than that of unirradiated ECO. This is surprising because it implies that the material becomes not only more brittle and stiffer but also stronger (undesirable in enhanced degradable polymers) with the irradiation time. It also clearly indicates that there are substantial differences, albeit unknown in detail, between the ECO used in the studies of Lambros et al.,<sup>11</sup> Li et al.,<sup>13</sup> and this work. In our attempt to determine the possible reasons for these discrepancies, we were able to obtain a small sample of the material used by Lambros et al.,<sup>11</sup> and we performed DSC measurements on it. The results did not show significant differences between the two materials. However, this is not conclusive because the two materials could possess different molecular weights, oxygen contents, semicrystalline contents, and so forth. Nonetheless, the macroscopic differences are clear [Figs. 1 and 5(a)],

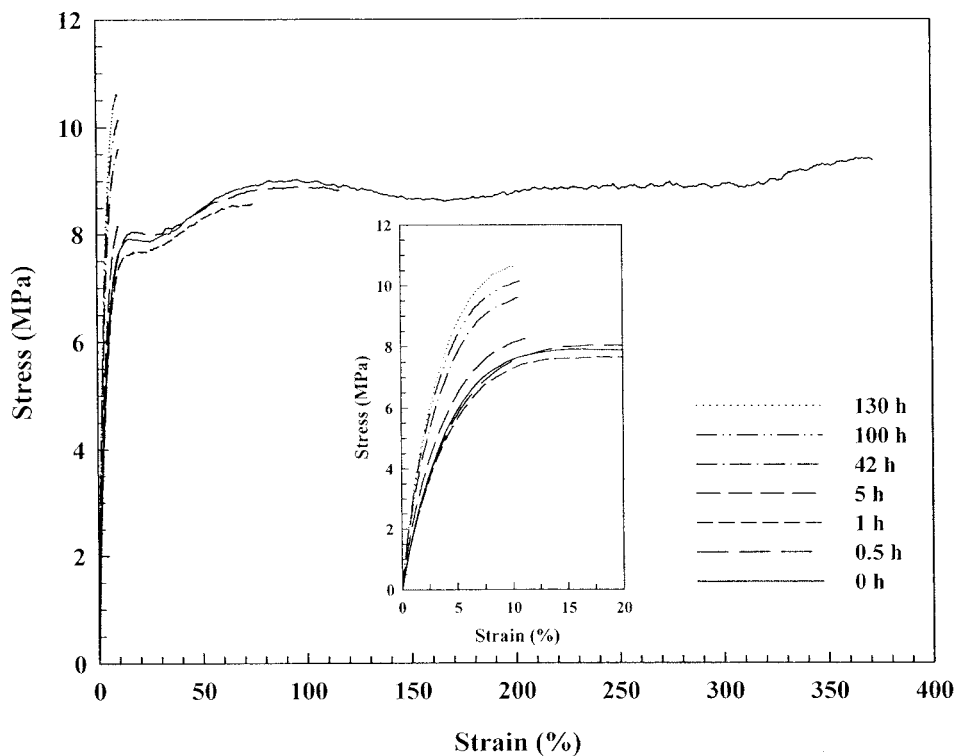
and they are expected to affect the material fracture response.

### Quasistatic crack growth resistance curves

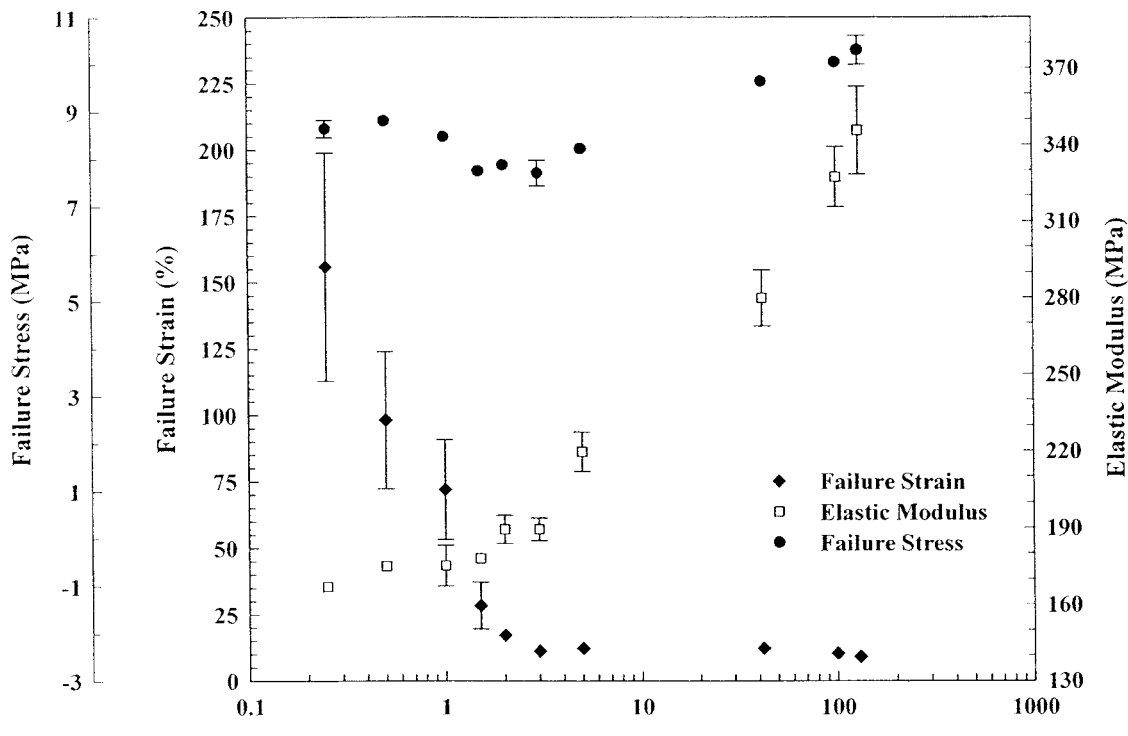
A complete understanding of the mechanical response of ECO, its susceptibility to UV degradation, and, by extension, its usefulness as an environmentally friendly enhanced degradable polymer includes the accurate determination of crack initiation and growth properties. To this end, fracture experiments following the protocol described earlier were performed on ECO specimens that were irradiated for 5, 42, and 130 h. Fracture tests were not performed on a material that was irradiated for times shorter than 5 h because it possessed extensive ductility and crack blunting was overwhelming. The fracture tests were analyzed with the full-field optical technique of DIC, which correlated a pair of digital images: one taken during the fracture event (deformed state) and one taken just before the test began (undeformed state). Six deformation parameters (the in-plane displacements  $u_x$  and  $u_y$  along the  $x$  and  $y$  directions, respectively, and the displacement gradients  $\partial u_x/\partial x$ ,  $\partial u_y/\partial y$ ,  $\partial u_x/\partial y$ , and  $\partial u_y/\partial x$ ) were directly obtained by this method. In each case, these six parameters were determined at 6561 points that were 0.303 mm apart in an area of 24.5 mm  $\times$  24.5 mm surrounding the propagating crack tip. A typical DIC result is presented in Figure 6, which shows the vectorial representation of the total displacement and the corresponding displacement gradient,  $\partial u_y/\partial y$  (i.e., normal strain in the direction of the applied displacement), for an ECO sample homogeneously irradiated for 42 h and subjected to an applied displacement of 3.21 mm. The current crack-tip position is at the origin, and the displacement vector length has been reduced to 0.3 of the actual length for viewing purposes. It is easy to see the symmetry of the normal strain [Fig. 6(b)] with respect to the  $x$  axis, typical of mode I loading, although such symmetry is lacking in Figure 6(a). The reason for this lack of symmetry in the displacement field is that in addition to displacements generated by the crack, a rigid body rotation and translation are superposed, and this destroys the symmetric crack-tip field. The rigid body motion does not affect the strain results in Figure 6(b), which involve a spatial derivative of displacement. When the rigid body motion is evaluated and removed, as described later, the displacement field also becomes symmetric (not shown).

For an isotropic linear elastic homogeneous material containing a crack, the opening displacement  $u_y$  is given asymptotically by

$$u_y = K_I \frac{\sqrt{r}}{\mu \sqrt{2\pi}} \sin \frac{\theta}{2} \left( \frac{2}{1+\nu} - \cos^2 \frac{\theta}{2} \right) + A_1 r \cos \theta + A_2 \quad (2)$$



(a)



(b)

**Figure 5** Uniaxial tensile test results: (a) the effect of the UV-irradiation time on the stress–strain response of ECO and (b) the average values of the failure strain, failure stress, and elastic modulus as a function of the UV-irradiation time. At least three specimens were tested for every irradiation time, and the scale was chosen to visually separate the three quantities.

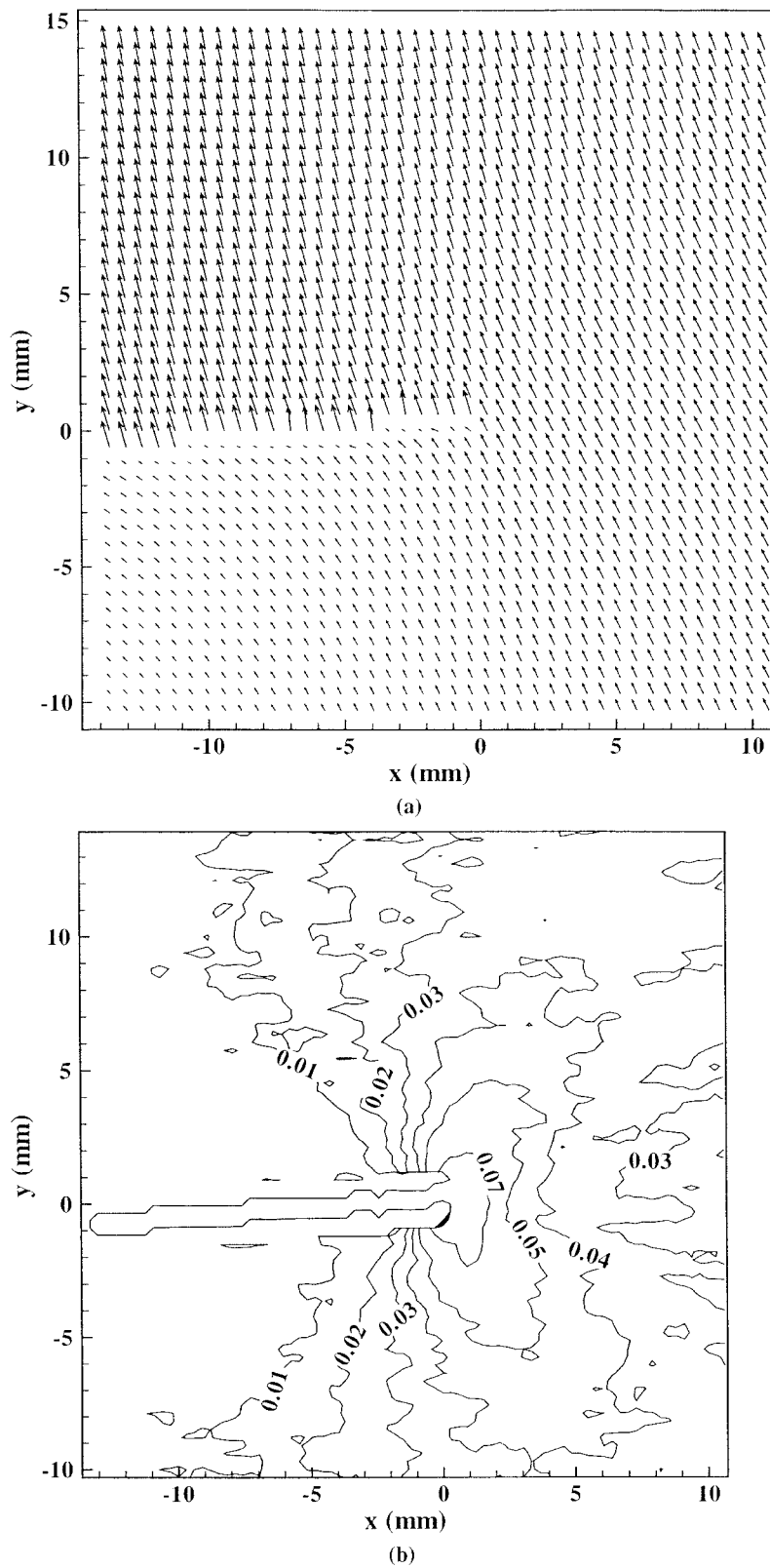


**Figure 6** DIC measurements from a fracture test performed on a 42-h ECO specimen under an applied displacement of 3.21 mm: (a) the displacement vector (so that overlapping would be avoided, only every other vector in both directions was plotted) and (b) the contour plot of the normal strain in the  $y$  direction. The current crack-tip position in both plots is at the origin.



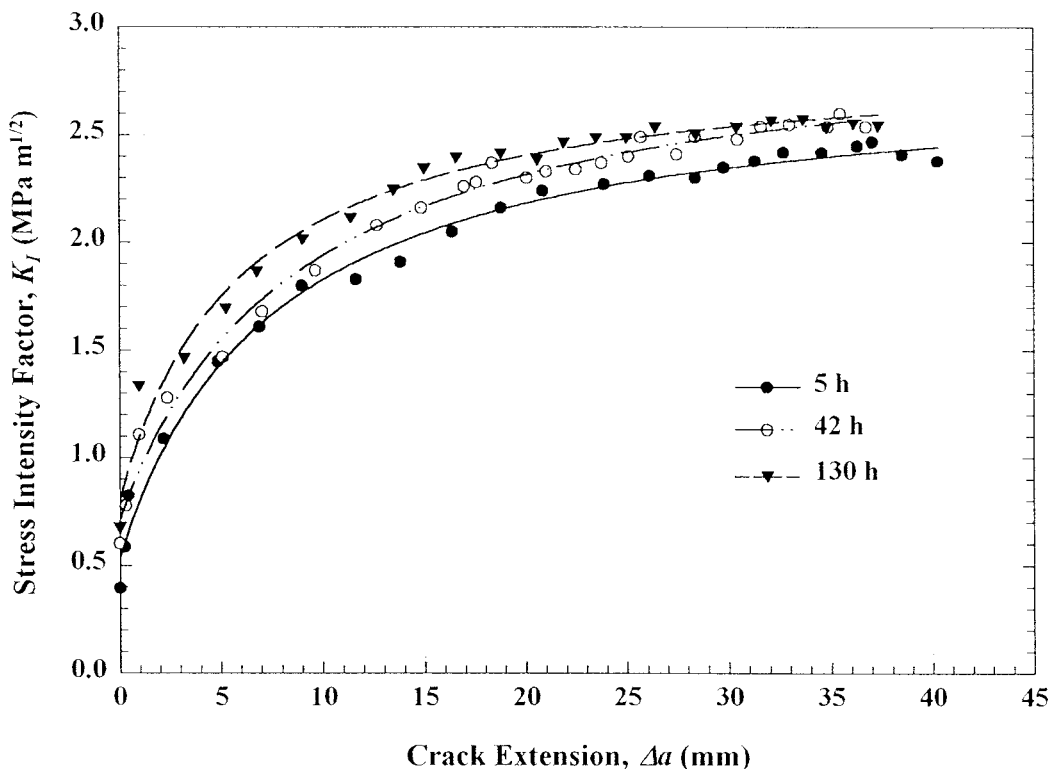


**Figure 7** Resistance curves for 1 wt % CO ECO after it was UV-irradiated for 5, 42, and 130 h, as determined by DIC. A fitting curve was added for every UV-irradiation time.

where  $\mu$  and  $\nu$  are the material shear modulus and Poisson's ratio, respectively, and  $r$  and  $\theta$  are polar coordinates centered at the crack tip (see Fig. 3). The first term on the right-hand side is the displacement in the  $y$  direction generated by the presence of the crack,<sup>19</sup> whereas the remaining two terms represent the rigid body rotation and translation of magnitudes  $A_1$  and  $A_2$ , respectively. The values of  $K_I$  and rigid body constants  $A_1$  and  $A_2$  can be obtained from the least-squared minimization of eq. (2) and the full-field DIC-measured  $u_y$  displacement [Fig. 6(a)].

For all fracture tests, deformed images, at about 25 different crack lengths, were correlated with the corresponding undeformed ones, and this yielded measurements of  $K_I$  as the crack grew. Crack growth resistance curves plotting the evolution of  $K_I$  versus  $\Delta a$  for three different irradiation times (5, 42, and 130 h) are presented in Figure 7. All three curves show almost the same functional behavior, and this is typical of quasibrittle homogeneous materials. The validity of using eq. (2) to model the material used in the current study was investigated by Li et al.<sup>13</sup> and Abanto-Bueno and Lambros.<sup>15</sup> For small values of  $\Delta a$  ( $\leq 5$  mm), the toughness of irradiated ECO increases, and this increase is typically associated with crack blunting. As the crack grows further ( $\Delta a > 5$  mm), the toughness increases but in a less pronounced fashion and finally reaches an almost constant value (plateau)

for continued crack growth in which steady-state conditions have been achieved.

The more surprising aspect of the results of Figure 7 resides in the fact that the toughness of ECO actually increases with increasing irradiation time (5–130 h), in direct contrast to the results shown in Figure 2 (Li et al.<sup>13</sup>). Thus, ECO becomes tougher with increasing UV-irradiation exposure, even though this is not a monotonic increase over the entire irradiation range because either in an unirradiated state or for irradiation times of less than 5 h, it is very difficult to propagate a crack. Recall that no fracture tests were performed below 5 h and that for those irradiation periods failure strain was much larger than 10%. Nonetheless, it is important to recognize that upon prolonged irradiation, this particular material, which clearly differs from that tested in Li et al.,<sup>13</sup> does strengthen. This is generally undesirable in a photo-degradable environmentally friendly material, and as suggested by Narayan,<sup>20</sup> any use of this material as such should be done not only on the basis of its documented embrittlement but also on the higher toughness values obtained upon continued irradiation.

Even though they contradict the results of Li et al.<sup>13</sup> (Fig. 2), the resistance curves obtained in this work (Fig. 7) can be explained when analyzed in conjunction with the corresponding material constitutive re-

sponse [Fig. 5(a)]. For irradiation times exceeding 5 h, the material exhibits an increasing failure stress and an almost invariable failure strain. If the failure mechanism is controlled by a critical strain level, which is the case for polymer crazing, that is, the failure mechanism exhibited by ECO, as the UV irradiation increases, the critical failure strain will be attained at higher and higher stress levels. Therefore (with the possible exception of irradiation periods of less than 5 h), as the irradiation time increases, the material is able to absorb more energy (a larger area under the stress-strain curve), and so the material fracture toughness increases (Fig. 7). This mechanism is similar to the strain rate toughening of rate-dependent solids that fail by a strain-controlled mechanism.<sup>21</sup>

### CONCLUSIONS

In this work, the effect of UV irradiation on the uniaxial mechanical properties and fracture behavior of 1 wt % CO ECO was studied with uniaxial tensile tests and companion fracture tests. The full-field DIC technique was used to measure the in-plane deformation during the fracture experiments. Average values of the failure strain, failure stress, and elastic modulus were determined from the tensile tests. The elastic modulus always increased with UV irradiation. In addition, for early irradiation times of less than 5 h, both the failure strain and failure stress of ECO decreased, the former drastically, the latter less so. For longer irradiation times, the failure strain remained almost invariable, but surprisingly, the failure stress increased by about 25% over the value of unirradiated ECO. As a result of a strain-controlled failure process such as crazing, this increase in the stress levels resulted in a material that toughened for irradiation times exceeding 5 h. This toughening was directly measured by a comparison of the resistance curves of ECO irradiated at 5, 42, and 130 h, which showed an increasing resistance to fracture as the UV-irradiation time increased. Therefore, in conclusion, we can say

that for longer irradiation times (>5 h), 1 wt % CO ECO becomes not only stiffer but also stronger and tougher.

The Hi-Cone Division of Illinois Tools Work Co. generously provided the material.

### References

1. Andrady, A. L. *J Appl Polym Sci* 1990, 39, 363.
2. Hartley, G. H.; Guillet, J. E. *Macromolecules* 1968, 1, 165.
3. Heskins, M.; Guillet, J. E. *Macromolecules* 1970, 3, 224.
4. Li, S. K. L.; Guillet, J. E. *J Polym Sci Polym Chem Ed* 1980, 18, 2221.
5. Torikai, A.; Takeuchi, A.; Nagaya, S.; Fueki, K. *Polym Photochem* 1986, 7, 199.
6. Nakatsuka, S.; Andrady, A. *J Environ Polym Degrad* 1994, 2, 161.
7. Furneaux, G. C.; Ledbury, K. J.; Davis, A. *Polym Degrad Stab* 1981, 3, 431.
8. Andrady, A. L.; Pegram, J. E.; Nakatsuka, S. *J Environ Polym Degrad* 1993, 1, 31.
9. Andrady, A. L.; Pegram, J. E.; Searle, N. D. *J Appl Polym Sci* 1996, 62, 1457.
10. Li, R.; Wu, S.; Ivanova, E.; Chudnovsky, A.; Sehanobish, K.; Bosnyak, C. P. *J Appl Polym Sci* 1993, 50, 1233.
11. Lambros, J.; Santare, M. H.; Li, H.; Sapna, G. H., III. *Exp Mech* 1999, 39, 184.
12. Ivanova, E.; Chudnovsky, A.; Wu, S.; Sehanobish, K.; Bosnyak, C. P. *Exp Tech* 1996, 20, 11.
13. Li, H.; Lambros, J.; Cheeseman, B. A.; Santare, M. H. *Int J Solids Struct* 2000, 37, 3715.
14. Domininghaus, H. *Plastic for Engineers: Materials, Properties and Applications*; Hanser: Munich, 1993.
15. Abanto-Bueno, J.; Lambros, J. *Eng Fract Mech* 2002, 69, 1695.
16. Sutton, M. A.; Wolters, W. J.; Peters, W. H.; Ranson, W. F.; McNeill, S. R. *Image Vision Comput* 1983, 1, 133.
17. Bruck, H. A.; McNeill, S. R.; Sutton, M. A.; Peters, W. H., III. *Exp Mech* 1989, 29, 261.
18. Vendroux, G.; Knauss, W. G. *Exp Mech* 1998, 38, 86.
19. Eftis, J.; Subramonian, N.; Liebowitz, H. *Eng Fract Mech* 1977, 9, 189.
20. Narayan, R. In *Opportunities for Innovation: Biotechnology*; Busche, R. M., Ed.; NIST GCR 93-633; National Institute of Standards and Technology: Gaithersburg, MD, 1993.
21. Freund, L. B. *Dynamic Fracture Mechanics*; Cambridge University Press: Cambridge, England, 1990.